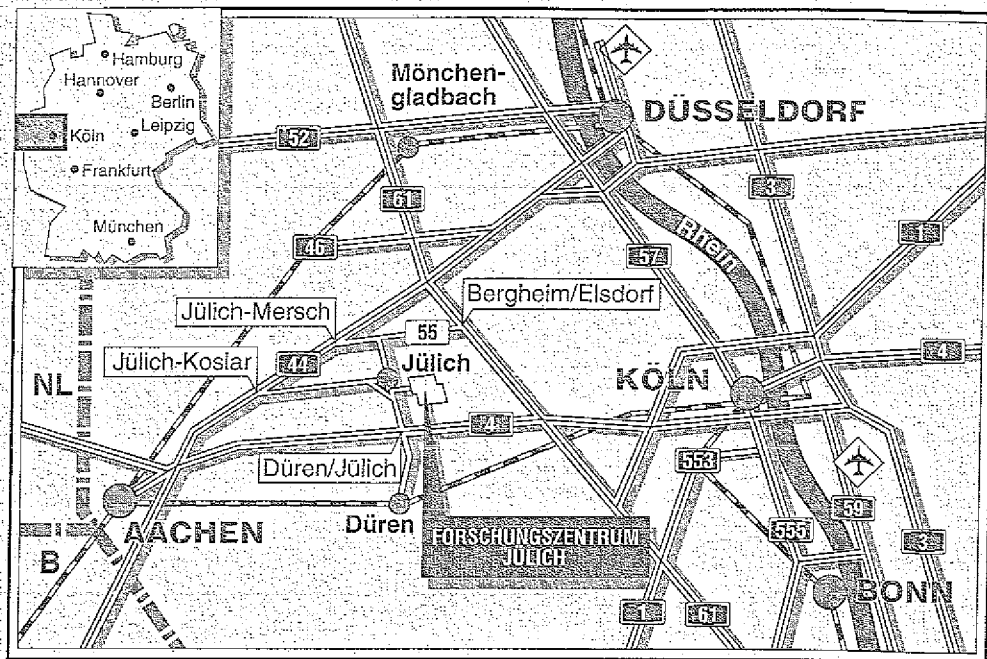


*Institut für Chemie und Dynamik der Geosphäre 3
Institut für Festkörperforschung*

**Nonlinearities in the Gas Phase
Chemistry of the Troposphere:
Oscillating Concentrations
in a Simplified Mechanism**

D. Poppe H. Lustfeld



Berichte des Forschungszentrums Jülich ; 3011

ISSN 0944-2952

Institut für Chemie und Dynamik der Geosphäre 3 Jül-3011

Institut für Festkörperforschung

Zu beziehen durch : Forschungszentrum Jülich GmbH · Zentralbibliothek

D-52425 Jülich · Bundesrepublik Deutschland

Telefon : 02461/61-6102 · Telefax : 02461/61-6103 · Telex : 833556-70 kfa d

Nonlinearities in the Gas Phase Chemistry of the Troposphere: Oscillating Concentrations in a Simplified Mechanism

D. Poppe¹ H. Lustfeld²

¹Institut für Chemie und Dynamik der Geosphäre 3: Atmosphärische Chemie

²Institut für Festkörperforschung

100% of the total population
of the world are to be included
in the total population of the
world. The total population of the
world is 6.5 billion.

100% of the total population

Abstract

The nonlinear coupling of atmospheric trace constituents can - at least in principle - cause concentrations to oscillate with time. This is demonstrated for a simplified scheme encompassing only the tropospheric gas phase chemistry of CO, O₃, HO_x, and NO_x. Oscillating concentrations with a common period of about 33 d were found for all chemical compounds under the forcing by time independent sources for CO and NO. Linear stability analysis shows that already the linearized system has complex time constants. Thus even the linearized system can oscillate. Since the periodic solution is a stable attractor, this type of solution persists, even when perturbed by atmospheric mixing or dilution. The presence of methane or an external source of ozone destroys the oscillation. This finding limits the applicability for problems of the real atmosphere. The source strengths of NO and CO necessary to produce undamped oscillations in the model are much larger than the corresponding globally averaged source strengths. In the polluted boundary layer, however, the source strengths of NO and CO could very well be encountered. Evaluation of the Lyapunow exponents and of the dependence on the initial conditions indicate that the periodic solution is attained usually within a few days. Thus, even if the meteorological and source strength conditions do not persist for the time of a whole period parts of it may still be observable.

1. Introduction

Nonlinear processes in dynamical systems have gained a large deal of attention during recent years. In atmospheric chemistry it has been shown that nonlinear couplings give rise to multiple steady states (White and Dietz, 1984, Kasting and Ackerman, 1985, Madronich and Hess, 1994) and to bifurcations (Zimmermann and Poppe, 1993).

The purpose of the present paper is to explore further the existence and behaviour of nonlinear phenomena in the gasphase chemistry of the troposphere. Many reactions are bimolecular. Thus their chemical reaction rates depend on the products of two reactand concentrations, which leads to evidently nonlinear terms in the balance equations of the reactands. If the life times of the reactands are markedly different the nonlinearity may not be of importance. For example, the reaction of methane with the OH radical is a nonlinear process. However, due to the long life time of CH_4 of several years the reaction is virtually a linear process as long as the time scale of interest is small compared to the atmospheric life time of methane.

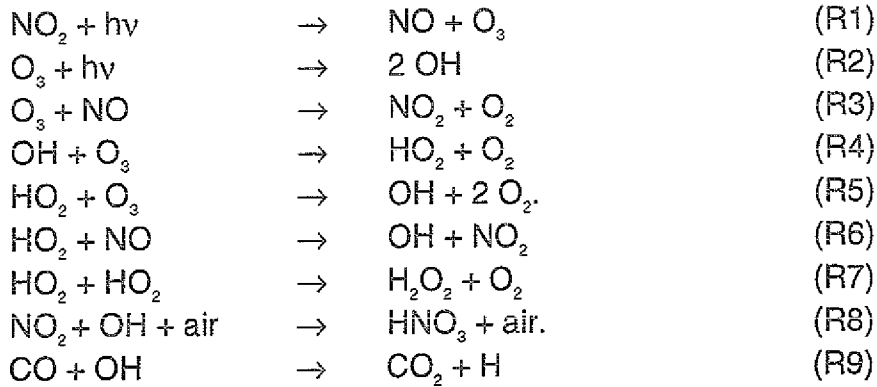
The goal of this first approach is an explorative study of the possible consequences of nonlinear processes in a reaction scheme that contains just enough reactions to describe the salient features of tropospheric photochemistry. This precludes, of course, the applicability of the findings to the real atmosphere. However, we will assess the constraints under which these oscillatory behaviour might be experimentally observable.

2. A reduced reaction scheme of the day time atmospheric chemistry

In order to explore the nonlinear properties of the gas phase chemistry we restrict ourselves to a small set of reactions, that encompasses the generic features of the fast photo chemistry thereby omitting parallel reactions and processes that do not exhibit significant rates. This simplified fast photochemistry consists of reactions of OH, HO_2 , NO, NO_2 , and O_3 . Only CO as a representative of oxidizable compounds is

included. Also we omit the reaction of OH with HO₂ though it has a substantial influence on the actual concentrations. It is generically represented by the self reaction of HO₂. The reaction scheme is compiled in table 1.

Table 1: Simplified reaction scheme



Extremely shortlived compounds like O¹D, O³P, and H are treated as steady state species. Longlived products like H₂O₂ and HNO₃ that have negligible influence during time period considered were not included. First order losses of NO_x with a decay constant $k = 5 \cdot 10^{-6} \text{ sec}^{-1}$ are also included. Photolysis frequencies $k_1 = 9.0 \cdot 10^{-3} \text{ s}^{-1}$, $k_2 = 2.66 \cdot 10^{-6} \text{ s}^{-1}$. All other rate constants were taken from Stockwell et al. 1990. Density of air is $2.5 \cdot 10^{19} \text{ cm}^{-3}$.

The balance equations read

$$\begin{aligned}
 d[\text{NO}_2]/dt &= -F_1 && +F_3 && +F_6 && -F_8 && (1) \\
 d[\text{O}_3]/dt &= && -F_2 && -F_3 && -F_4 && -F_5 \\
 d[\text{NO}]/dt &= && F_1 && -F_3 && -F_6 && +Q(\text{NO}) \\
 d[\text{CO}]/dt &= && && && -F_9 && +Q(\text{CO}) \\
 d[\text{OH}]/dt &= && 2F_2 && -F_4 && +F_5 && +F_6 && -F_8 && -F_9 \\
 d[\text{HO}_2]/dt &= && && +F_4 && -F_5 && -F_6 && -2F_7 && +F_8
 \end{aligned}$$

where F_i is the rate of reaction Ri.

The time scale of the system is given by the compounds with the large life times i.e. CO and ozone. The short term behaviour is governed by the life time of OH and HO_x (= HO₂ + OH) of 1 sec and up to 1 min, resp. Reactions that are only important during the night are not included. Also time dependence of HNO₃ and H₂O₂ is not

considered since their possible chemical feed back through photolysis and reactions with OH are not significant on the time scale under consideration. In dependence on source terms for CO and NO, $Q(\text{CO})$ and $Q(\text{NO})$, the systems undergo dramatic changes in its temporal development. Both the photolytic dissociation of ozone and NO_2 , R1 and R2 (see table 1), and these sources are the driving forces of the reaction system. Since the rates are linear or quadratic functions of the concentrations, eqs (1) are a set of nonlinear ordinary differential equations. They have to be solved numerically.

3. The fixed point equations

Linearisation of the equations of motion of a system can provide useful information on the dynamical behaviour, the response to perturbations, and the characteristic time constants of the system. The inherent nonlinear features and the overall behaviour, however, cannot be found from such an analysis. The conceptual appeal of the linear approximation is the availability of a large body of rigorous mathematical results on the behaviour of such systems (see for example, Gray and Scott, 1994).

First we rewrite eqs (1) in the form

$$d C_i / dt = f_i(C_1, \dots, C_n) \quad (2)$$

or in vectorized form

$$d \mathbf{C} / dt = \mathbf{f}(\mathbf{C}) \quad (3)$$

where \mathbf{C} denotes the vector of concentrations (C_1, \dots, C_n) and \mathbf{f} the right hand side of eq(2) $(f_1(C_1, \dots, C_n), \dots, f_n(C_1, \dots, C_n))$. In this and the following section we discuss the local and global behaviour of the system eqs (1) in the six dimensional vector space of all concentrations. "Local" addresses the properties of the motion in the vicinity of a point \mathbf{C} on time intervals small compared to the time under consideration, where the linearization is approximately valid and provides meaningful results. The term

"global" encompasses the long term development and the general pattern of motion beyond the validity of a linearized approach.

The initial step is a Taylor expansion of eq (3) up to first order at a given point

$$\mathbf{C}_0 = \mathbf{C}(t_0)$$

$$dy/dt = f(\mathbf{C}_0) + \mathbf{A}(\mathbf{C}_0) \mathbf{y} \quad (4)$$

where $\mathbf{y} = \mathbf{C} - \mathbf{C}_0$ and \mathbf{A} is the Jacobian matrix. Its elements are the partial derivatives of \mathbf{A} at \mathbf{C}_0 .

$$A_{ik} = (\partial f_i / \partial C_k) \quad (5)$$

Within the validity of the linear approach the development in time for a time independent \mathbf{A} can be easily deduced. The eigenvalues of the Jacobian are characteristic for the time constants of the system. If we denote the eigenvalues by a_i , the temporal evolution is given by a linear combination of exponentials of the form $\exp(a_i t)$. Since the Jacobian \mathbf{A} is in general not a symmetric matrix the eigenvalues are not necessarily real. If all eigenvalues a_i have negative real parts the system is called stable and reaches asymptotically a stable stationary state or a fix point \mathbf{C}_s defined by $f(\mathbf{C}_s) = 0$. Then the eigenvalue with the largest real part determines the typical time T to attain the stationary state.

$$T = -1/\max(\operatorname{Re} a_i) \quad (6)$$

Non vanishing imaginary parts, which occur pairwise with opposite sign due to the reality of \mathbf{A} , cause oscillations. The frequency ω is given by

$$\omega = \operatorname{Im} a_i \quad (7)$$

If at least one eigenvalue has a positive real part the system is unstable with exponentially growing concentrations.

The matrix \mathbf{S} of the eigenvectors of \mathbf{A} contains information on the compounds that are associated with a given time constant. More precisely, the linear combination $\sum S_{ij}^{-1} C_j$ decays exponentially with the time constant a_i . This analysis provides a

mathematically sound argument for the separation of fast and slow modes and also a consistent definition of chemical families. For a nonlinear system \mathbf{A} depends the concentrations \mathbf{C} and therefore implicitly on time.

4. Oscillatory solutions

In this section we wish to classify the types of solutions of eqs (1). For simplicity we introduce diurnally averaged photolysis frequencies for R1 and R2 (see table 1). In figure 1 numerical solutions for the standard case defined by $Q(\text{NO}) = 10^6 \text{ cm}^{-3}$ and $Q(\text{CO}) = 1.3 \cdot 10^6 \text{ cm}^{-3}$ are shown.

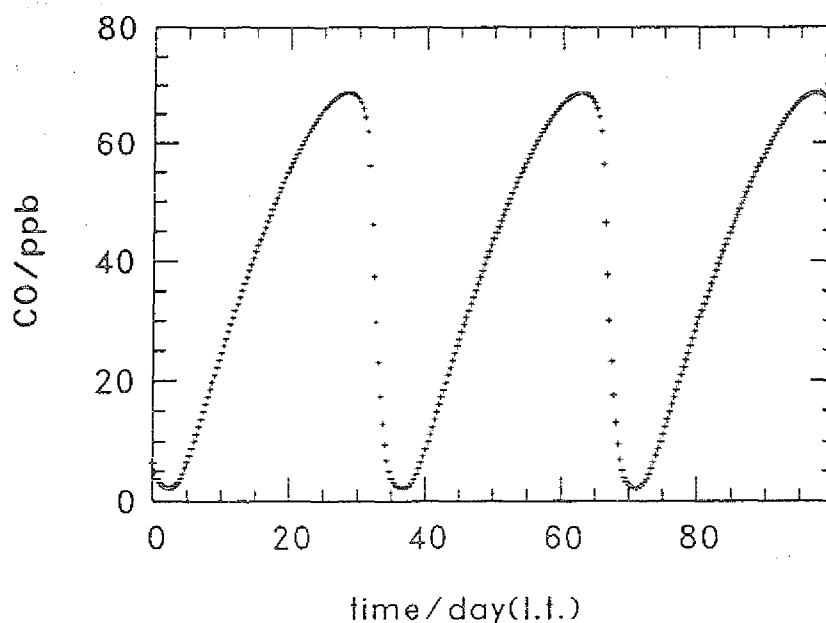


Figure 1a: Time dependence of the mixing ratio of CO for the standard case, $Q(\text{NO}) = 10^6 \text{ cm}^{-3} \text{ s}^{-1}$, $Q(\text{CO}) = 1.3 \cdot 10^6 \text{ cm}^{-3} \text{ s}^{-1}$.

The concentrations oscillate with a common frequency of about 33 days. Interestingly there is no indication of the influence of other frequencies, though in principle the linearized equations allow for up to three different periods.

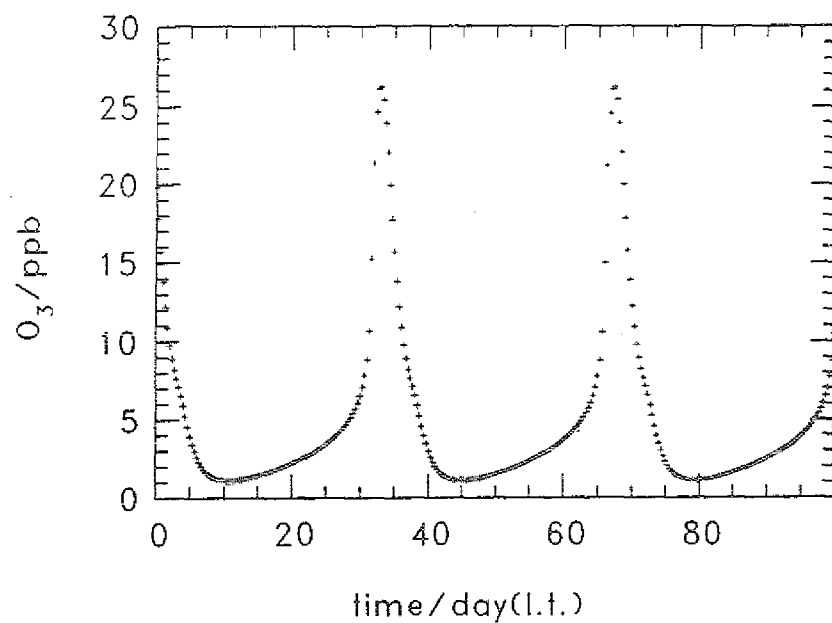


Figure 1b: Time dependence of the mixing ratio of O_3 for the standard case, $Q(\text{NO}) = 10^6 \text{ cm}^3 \text{ s}^{-1}$, $Q(\text{CO}) = 1.3 \cdot 10^6 \text{ cm}^3 \text{ s}^{-1}$.

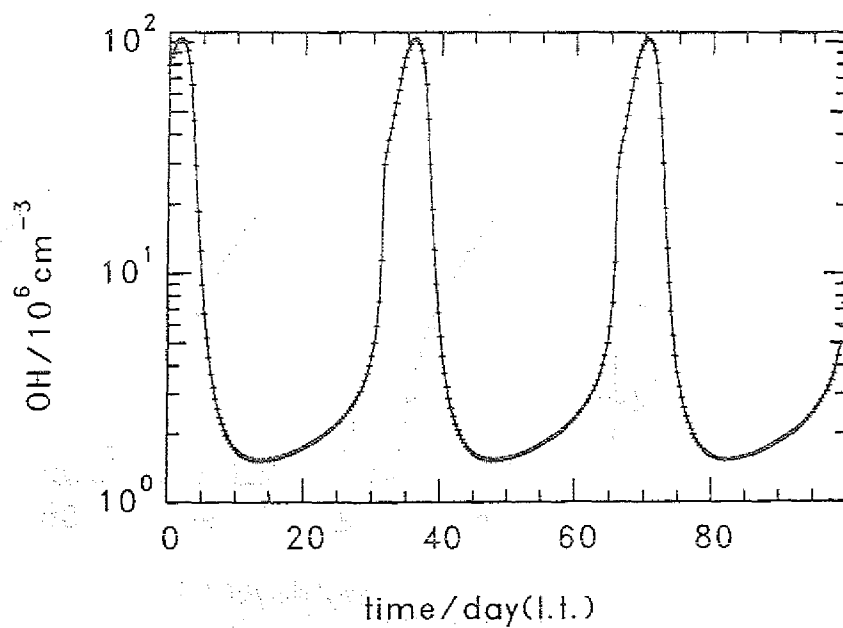


Figure 1c: Time dependence of the concentration of OH for the standard case, $Q(\text{NO}) = 10^6 \text{ cm}^3 \text{ s}^{-1}$, $Q(\text{CO}) = 1.3 \cdot 10^6 \text{ cm}^3 \text{ s}^{-1}$.

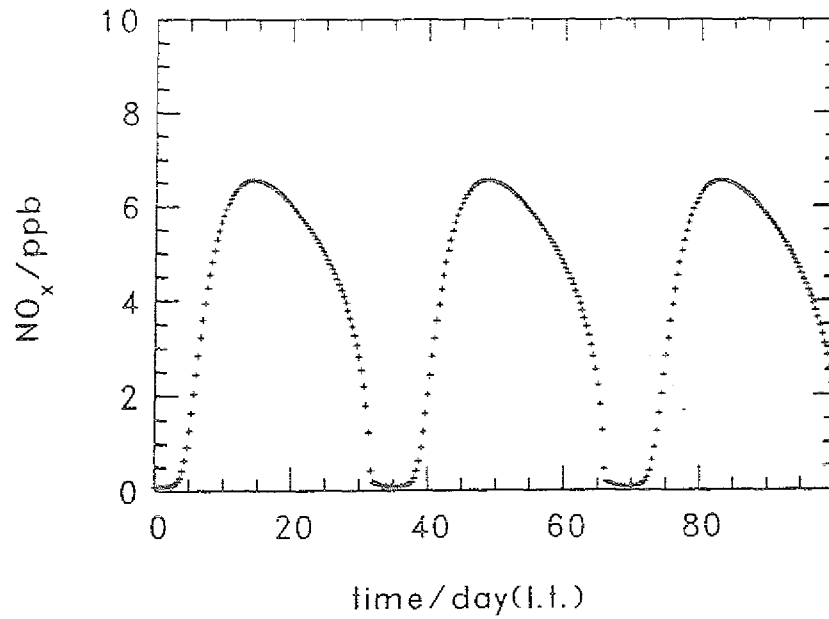


Figure 1d: Time dependence of the mixing ratio of NO_x for the standard case, $Q(\text{NO}) = 10^6 \text{ cm}^3 \text{ s}^{-1}$, $Q(\text{CO}) = 1.3 \cdot 10^6 \text{ cm}^3 \text{ s}^{-1}$.

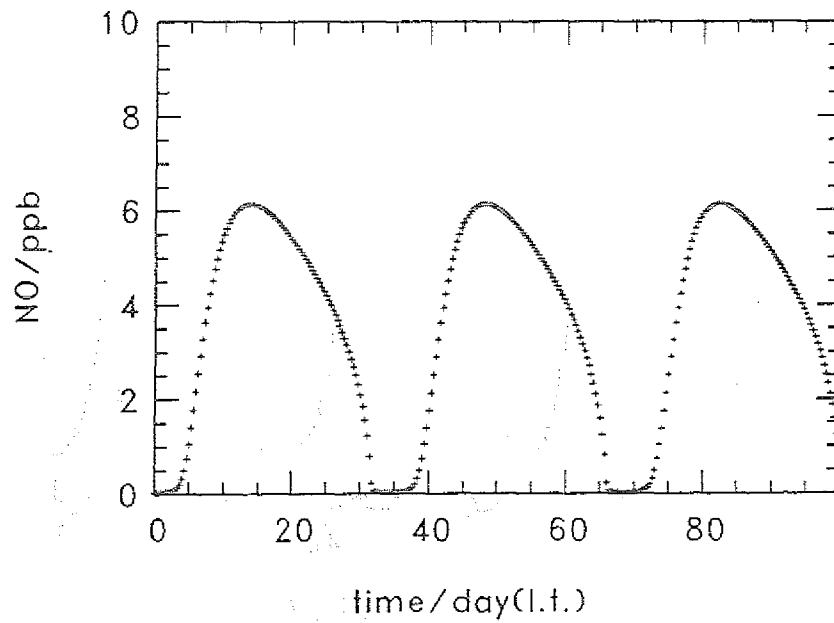


Figure 1e: Time dependence of the mixing ratio of NO for the standard case, $Q(\text{NO}) = 10^6 \text{ cm}^3 \text{ s}^{-1}$, $Q(\text{CO}) = 1.3 \cdot 10^6 \text{ cm}^3 \text{ s}^{-1}$.

The rates of all reactions undergo considerable changes during time as is shown in figure 2 for the standard case. In particular when [CO] steeply decreases all rates are comparable explaining also the strong nonlinear coupling during this time period.

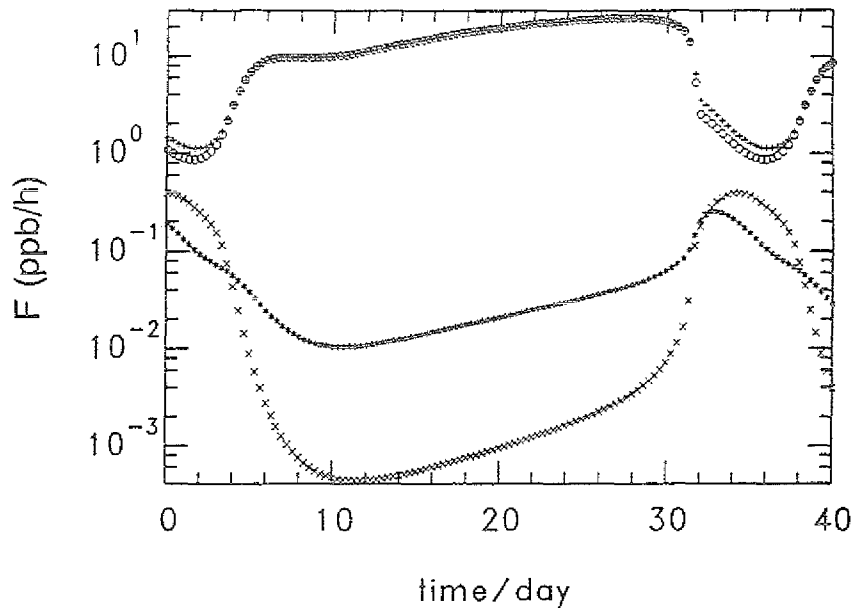


Figure 2a: Rates of reactions in units of ppb/h for the standard case. $R1=+$, $R2=*$, $R3=\circ$, $R4=\times$. The reactions R_i are listed in table 1.

Note that the maximum concentrations are attained at different times which can be attributed to the kinetic equations (1). For example at the maximum of [CO] at, say, t_m the first derivative with respect to time is zero, while the second derivative

$$d^2[\text{CO}]/dt^2 = -k_9 d[\text{OH}]/dt [\text{CO}] - k_9 [\text{OH}] d[\text{CO}]/dt \quad (8)$$

is negative. Therefore $d[\text{OH}]/dt$ is necessarily positive at t_m implying an increasing OH concentration. The overall behaviour can be easily deduced from an intuitive chemical picture. We begin at $t = 8$ d when the OH concentration is small, the depletion of CO due to R_9 is slow, and the budget of CO is governed by the CO source leading to increasing [CO] until $t = 24$ d. The increase is accompanied by photochemical production of ozone which is readily photolysed via R_1 to produce

OH. This reaction chain is an amplifying positive feedback for OH and leads to a steep increase of the OH concentration during $t = 28 \text{ d} \dots 33 \text{ d}$. Simultaneously $[\text{HO}_2]$ and $[\text{OH}]$ increase.

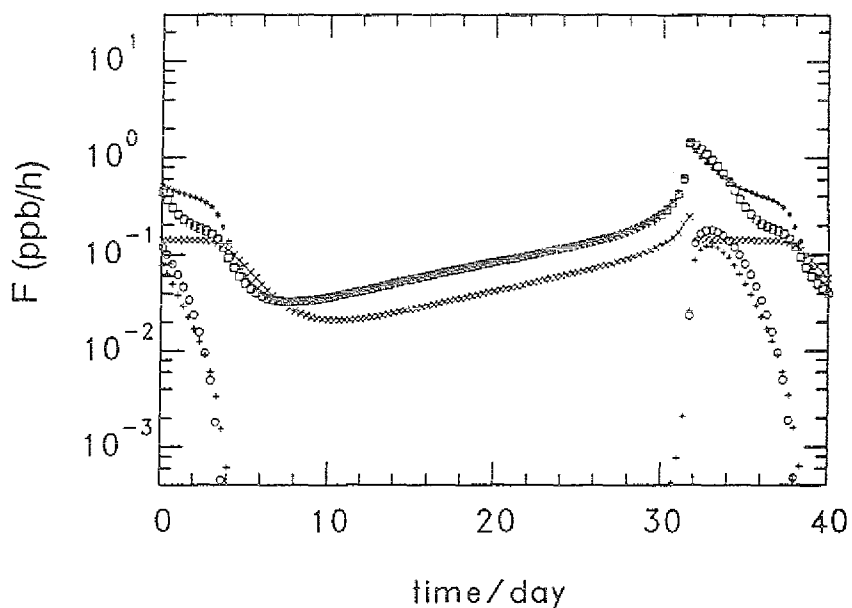


Figure 2b: Rates of reactions in units of ppb/h for the standard case. $R5=+$, $R6=*$, $R7=\circ$, $R8=x$, $R9=\square$. The reactions R_i are listed in table 1.

The latter quickly depletes CO, however, that does not lead to a corresponding net production of ozone since the NO concentration is small and, moreover, O_3 is efficiently destroyed in reactions R4 and R5 with OH and HO_2 . The short lived OH and HO_2 follow adiabatically the rapid decrease of its most important precursor. After about $\tau = 33 \text{ d}$ the cycle is completed. All components except NO_2 exhibit substantial amplitudes. Numerical tests with different initial conditions (however typical for atmospheric problems) have shown that the system approaches this oscillatory solution, i.e. this state is a stable attractor.

The occurrence of oscillations depends strongly on the relative strength of the CO- and NO-source. For $Q(\text{NO}) \ll Q(\text{CO})$ and also for $Q(\text{NO}) \gg Q(\text{CO})$ no oscillations

were observed. Apart from a short transient period the system approaches monotonically a stable state. In figure 3 a sequence of calculations for fixed $Q(\text{CO}) = 1.3 \cdot 10^6 \text{ cm}^3 \text{ s}^{-1}$ and varying $Q(\text{NO})$ is displayed. For $Q(\text{NO}) = 1.3 \cdot 10^6 \text{ cm}^3 \text{ s}^{-1}$ a damped oscillation is noticeable.

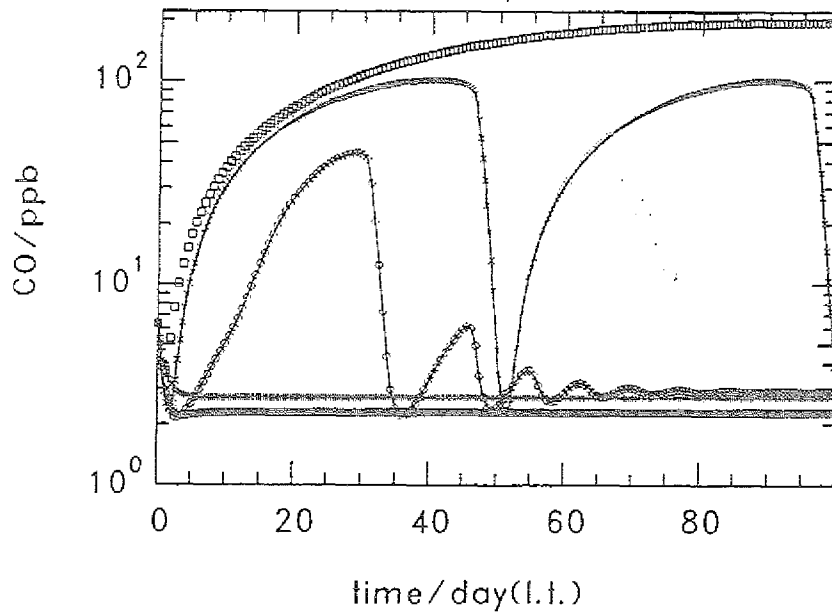
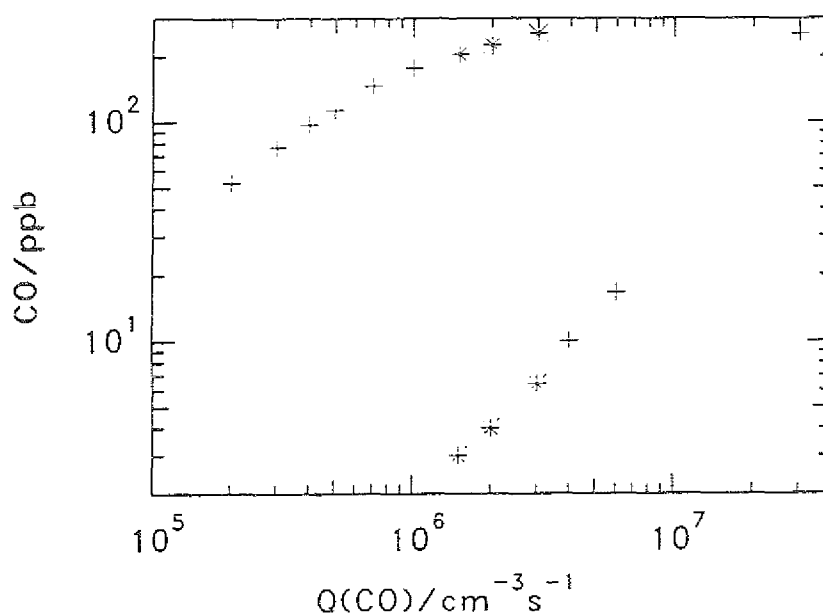


Figure 3: Time dependence of the CO mixing ratio for $Q(\text{CO}) = 1.3 \cdot 10^6 \text{ cm}^3 \text{ s}^{-1}$ and $Q(\text{NO}) = 3 \cdot 10^5 \text{ cm}^3 \text{ s}^{-1}$ (+), $Q(\text{NO}) = 6 \cdot 10^5 \text{ cm}^3 \text{ s}^{-1}$ (lowest curve), $Q(\text{NO}) = 7.851 \cdot 10^5 \text{ cm}^3 \text{ s}^{-1}$ (open circle), $Q(\text{NO}) = 1.3 \cdot 10^6 \text{ cm}^3 \text{ s}^{-1}$ (x), $Q(\text{NO}) = 2 \cdot 10^6 \text{ cm}^3 \text{ s}^{-1}$ (open square).

The system still approaches a steady state. With increasing $Q(\text{NO})$, however, the damping decreases until for $Q(\text{NO}) = 1.3 \cdot 10^6 \text{ cm}^3 \text{ s}^{-1}$ no damping is observed during the time of integration. Further increase of $Q(\text{NO})$ destroys the oscillation, thus for $Q(\text{NO}) = 2 \cdot 10^6 \text{ cm}^3 \text{ s}^{-1}$ a stationary state is approached. Steady state concentrations and extrema in case of oscillations indicate the dynamics of the process as function of the source strength $Q(\text{NO})$. For small $Q(\text{NO})$ the system has a stable steady state which becomes unstable if $Q(\text{NO})$ increases. The minima in the oscillatory regime is still in the vicinity of the stable state. The maxima is a measure of the developing stable steady state beyond the oscillatory domain. Similar results are found for CO

as function of $Q(\text{CO})$ for fixed $Q(\text{NO}) = 2 \cdot 10^6 \text{ cm}^3 \text{ s}^{-1}$ (figure 4). Note that small (large) source strengths of CO support large (small) steady state mixing ratios, which of course is directly related to the different OH abundances in the two regimes.



time constant of the HO_x family. Linear combinations for the other time constants do not have such an intuitive chemical interpretation, especially there is no mathematical evidence for $\text{NO}_x = \text{NO}_2 + \text{NO}$ to be a properly defined family. This finding proves the strong coupling between all compounds on comparable time scales.

During the simulation period only one pair of eigenvalues is complex, thus even the linearized system exhibits oscillations. Time domains associated with complex eigenvalues are characterised by having equal real parts. They can be easily identified in figure 5.

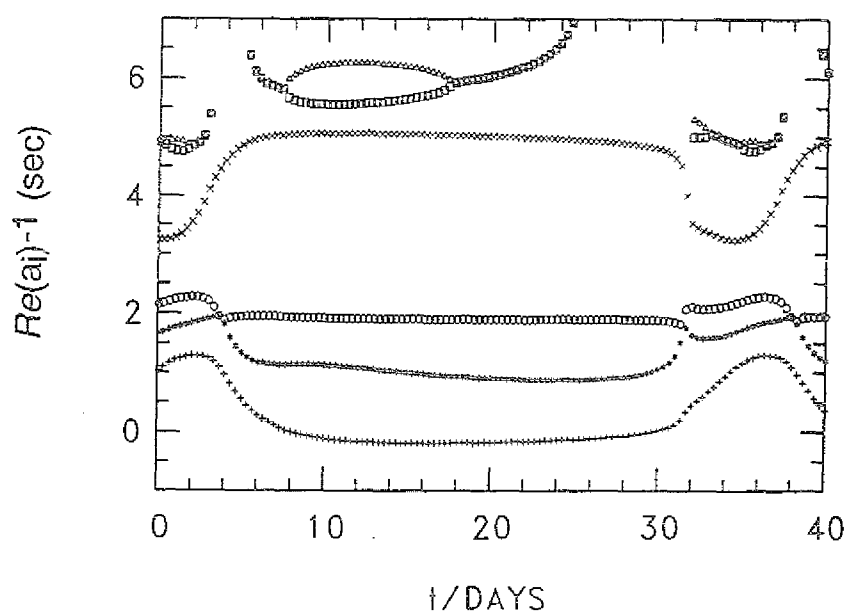


Figure 5a: Eigenvalues a_i of the Jacobian during the standard case. Entries correspond to the $\log(\text{base } 10)$ of time constants $= -1/\text{Re}(a_i)$ in units of sec if the real part is negative.

The imaginary parts (not shown in figure 5) vary only very little with time and correspond for the standard case to an oscillation period of 36 d, which is remarkably close to the periodicity of the nonlinear motion. Eigenvalues with positive real parts (figure 5b) are observed during the time of the OH maximum supporting the above discussed positive feedback within the system at this time.

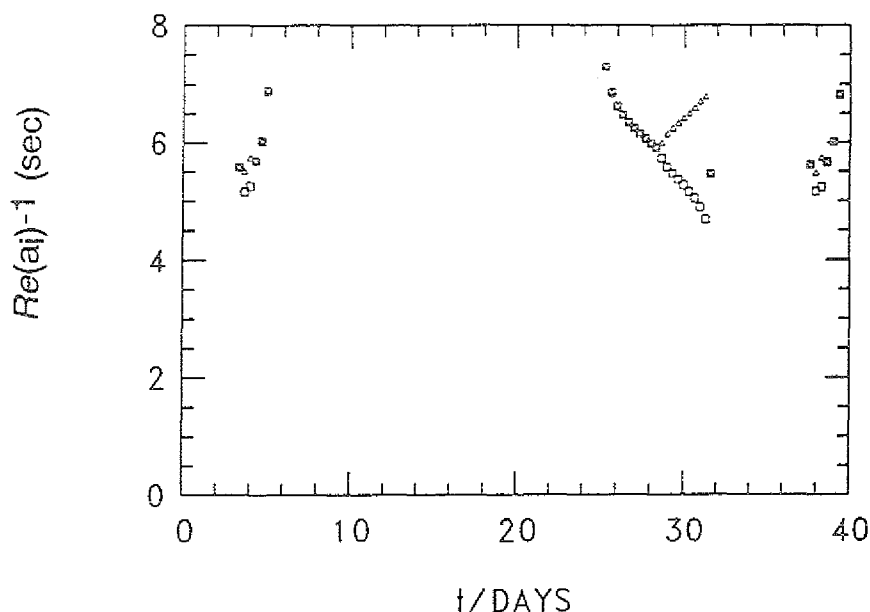


Figure 5b: Eigenvalues a_i of the Jacobian during the standard case. Entries correspond to the $\log(\text{base } 10)$ of time constants $= 1/\text{Re}(a_i)$ in units of sec if the real part is positive.

Since the eigenvalues of the Jacobian provide only with a local measure of stability in the space of concentrations at a given point $\mathbf{C}(t)$, we introduce the concept of Lyapunow exponents to investigate the overall stability of the oscillatory solution. The Lyapunow exponent (see for example Gray et al., 1994) is defined as a measure for the divergence or convergence of neighboring orbits in the space of concentrations as function of time: At time t_0 a (six dimensional) sphere with an infinitely small radius is put around $\mathbf{C}(t_0)$. As time continues this sphere is deformed to an ellipsoid defined by the requirement that all the trajectories started at t_0 in the sphere remain in the ellipsoid. As a consequence the axis of the ellipsoid $d_i(t)$ change with time and may be ordered

$$d_1(t) > d_2(t) > d_3(t) \dots$$

The local Lyapunow exponent $\lambda_i(t,s)$ expresses the rate of change of the radius d_i during the time interval s

$$\lambda_i(t,s) = (1/s) \ln (d_i(t)/(d_i(t-s))),$$

the global Lyapunow exponents are obtained by setting the time delay s equal to the period τ of the orbit. One global Lyapunow exponent is zero, since eqs (1) are an autonomous set of differential equations implying that two solutions $C(t)$ and $C(t+t_0)$ on the same periodic orbit remain in a finite distance in the six dimensional space of concentrations. Omitting this vanishing exponent, the stability is determined by the largest Lyapunow exponent, i.e. the periodic solution is stable if $\lambda_1 < 0$. Moreover the typical time T_{app} needed by a trajectory to approach the periodic solution in the stable regime is given by

$$T_{app} = -1 / \lambda_1$$

These results can also be used to investigate whether oscillating concentrations can be observed in the real atmosphere. Assume that the conditions, under which eqs (1) provide a meaningful description of the gas phase chemistry in a parcel of air, hold for a time window T_w . If $T_{app} \ll T_w$ then parts of the periodic orbit of the length T_w are observable. For example, if we consider the planetary boundary layer under stagnant high pressure conditions, this situation may last for $T_w = 1$ week on the average.

We have calculated the Lyapunow exponent for the standard case. To facilitate the numerics we invoked a steady state assumption for OH and HO₂ to eliminate the two negative very small Lyapunow exponents associated with these short lived species. Again disregarding the vanishing exponent we are left with only three λ_i corresponding to time constants $T_i (= -1/\lambda_i)$ of $T_1 = 6.3$ d, $T_2 = 3.2$ h, and $T_3 = 90$ sec. In fact from two directions in concentration space the periodic orbit is approached within several hours and minutes, resp. More critical is T_1 , therefore we have plotted $\lambda_1(t, T_w)$ as function of t along the orbit (figure 6).

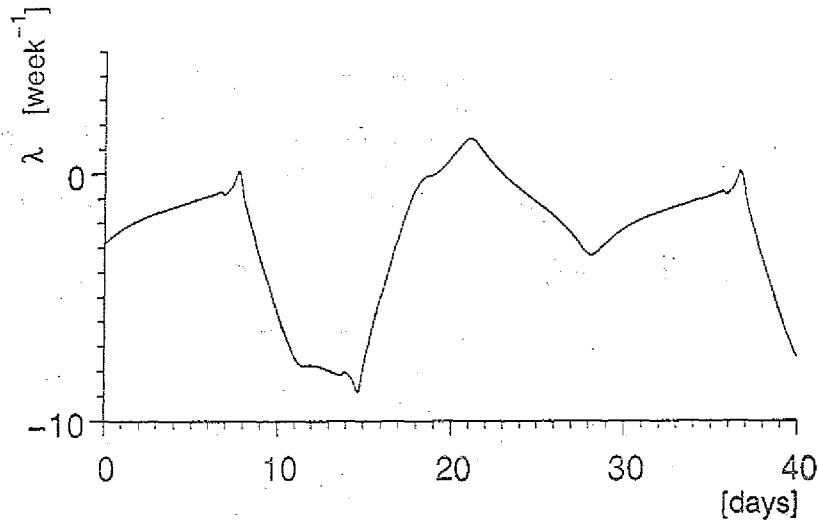


Figure 6: Time dependence of the largest Lyapunow exponent $\lambda_1(t, T_w)$ for the standard case.

Most of the time $-1/\lambda_1(t, T_w) < T_w$ indicating a compression of the ellipsoid at nearly all times. Thus the actual trajectory still follows the structure of the orbit. Therefore one should see parts of the orbit during windows in time of length T_w . This analysis proves the Lyapunow exponents are a useful tool in identifying whether periodic orbits can be seen in reality or not.

Eigenvalues of the Jacobian and the Lyapunow exponents characterize the local stability in concentration space. Another question is which initial conditions lead to trajectories that are finally attracted by the periodic solution and what are the time constants. We have recalculated the standard case, however, the initial conditions were taken randomly from $0.12 \text{ ppb} < \text{NO}_x < 300 \text{ ppb}$, $4 \text{ ppb} < \text{O}_3 < 100 \text{ ppb}$, and $0.3 \text{ ppb} < \text{CO} < 120 \text{ ppb}$. The initial concentrations of the short lived are not important. The results in figure 7a for CO generalizes the result from the (local) Lyapunow analysis that the periodic orbit is approached in about several days.

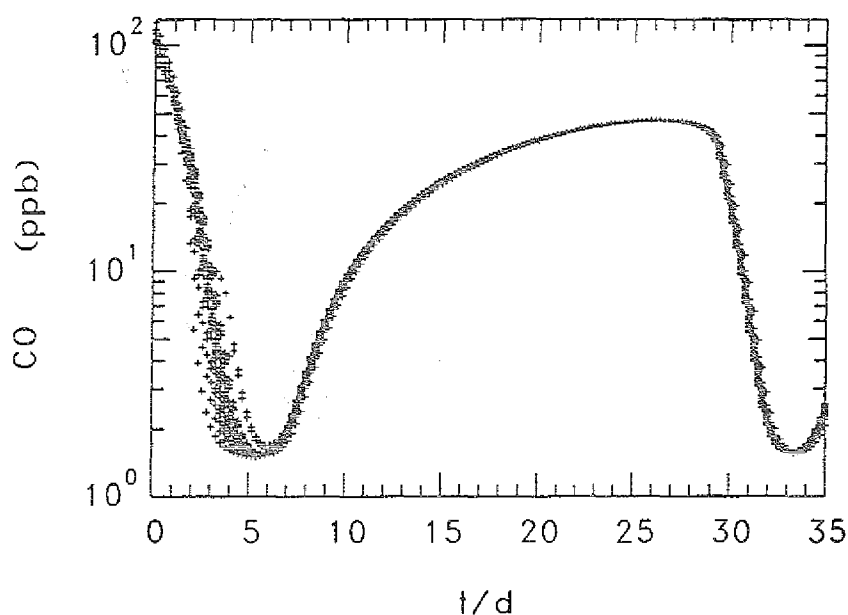


Figure 7a: Time dependence for 45 trajectories starting from different initial conditions (see section 5) under the standard case. The trajectories were shifted individually in time to have maximum overlap at $t > 20$ d, when all trajectories are on the orbit.

This is also found for ozone as the projection of the all trajectories on the CO-O_3 -plane in figure 7b demonstrates. Moreover this result suggests that the periodic orbit is a global attractor of the system, that is attained from virtually all atmospherically relevant initial conditions within several days.

The frequency and the amplitude of the apparently undamped oscillation for $Q(\text{NO}) = Q(\text{CO})$ depend on the source strength. The common value for $Q(\text{CO})$ and $Q(\text{NO})$ is denoted by Q . Increasing Q causes a decreasing frequency and an increasing amplitude. Also there is a threshold: the system does not exhibit undamped oscillations for $Q < 2 \cdot 10^5 \text{ cm}^3 \text{ s}^{-1}$. Damped oscillation were observed at even smaller source strengths.

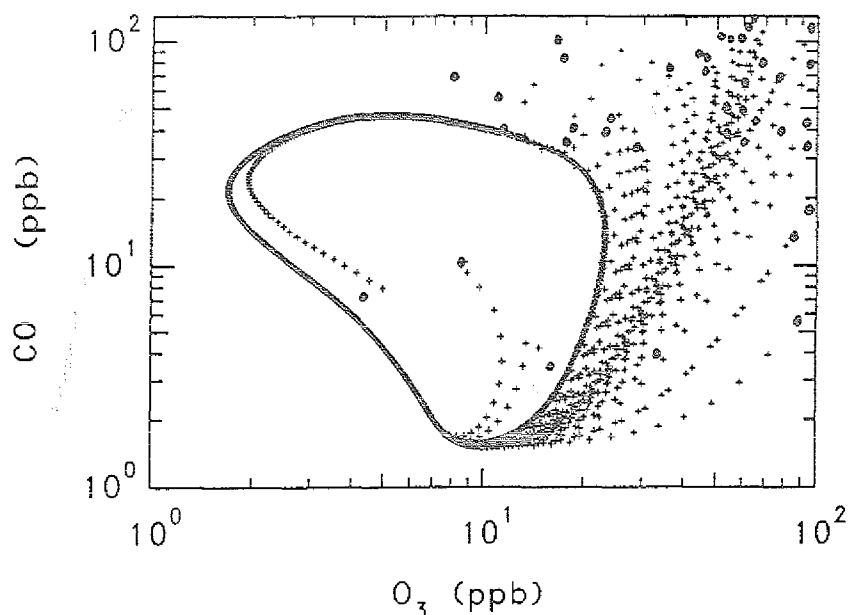


Figure 7b: Projection of these trajectories onto the O_3 -CO plane. The periodic orbit is attained from all trajectories. Initial conditions are indicated by full circles.

In order to address the effect of hydrocarbons that react faster with OH than CO we have introduced a somewhat artificial HC that reacts with OH in exactly the same way as CO, however, with a different reaction constant.



with $k_{10} = b k_9$

Calculations were done for $Q(NO) = 10^6 \text{ cm}^3 \text{ s}^{-1}$, $Q(HC) = 10^6 \text{ cm}^3 \text{ s}^{-1}$, and vanishing $Q(CO)$. One finds that the system still oscillates with a period and an amplitude that decreases with increasing b . Similar to the threshold for the sources there is an upper limit of the reaction constant, for $b > 7$ the oscillatory solution breaks down, since the time constants of ozone and NO_x are much larger than that of HC, so that

they cannot keep up oscillatory solutions. The shortest period observed was $T = 10$ d.

5. Application to Atmospheric Chemistry

Are these results of any relevance for the chemistry in the real atmosphere? In order to answer this question we have to address four problems. First, are the adopted source strength comparable to the known emissions of these compounds. Second, would atmospheric transport destroy the oscillatory behaviour. Third, do the oscillations persist if a more complex chemistry is included. Fourth, what is the influence of diurnally changing photolysis frequencies.

The global annual emissions of CO and NO_x are $2.7 \cdot 10^9$ t/a (as CO) and $5 \cdot 10^7$ t/a (as N) corresponding to emission strengths per unit of time and area $F(\text{CO}) = 3.6 \cdot 10^{11} \text{ cm}^2\text{s}^{-1}$ and $F(\text{NO}) = 1.3 \cdot 10^{10} \text{ cm}^2\text{s}^{-1}$, resp. Since most of the chemical processing occurs in the lower part of the troposphere (say at heights below 2 km) the globally averaged source strengths by volume are $Q(\text{CO}) = 1.8 \cdot 10^6 \text{ cm}^3\text{s}^{-1}$ and $Q(\text{NO}) = 6.7 \cdot 10^4 \text{ cm}^3\text{s}^{-1}$. Since $Q(\text{NO}) \ll Q(\text{CO})$ oscillations on the global scale are not to be expected. However, on the regional scale under stationary weather conditions and sources obeying $Q(\text{CO}) \sim Q(\text{NO})$ oscillation may evolve. The stationary conditions may not last long enough to experience the whole periodic orbit. However, since it is a stable attractor parts of the orbit may very well be present (see section 4).

Atmospheric transport causes additional terms in the balance equations. In order to explore the possible perturbations by dilution and mixing with air masses of different trace gas composition we employ a system of two boxes. In each of the boxes (denoted by 1 and 2) the chemistry of table 1 takes place. Transport of trace gases between the boxes is modeled by first order processes with the same time constant of exchange μ for all constituents. We chose $Q_1(\text{CO}) = Q_2(\text{NO}) = 0$, $Q_1(\text{NO}) = 10^6 \text{ cm}^3\text{s}^{-1}$, $Q_2(\text{CO}) = 1.3 \cdot 10^6 \text{ cm}^3\text{s}^{-1}$, which is similar to the standard case, however, the sources of NO and CO emit into different boxes. Not unexpected we

observe oscillations in box 1 if the time constant of the exchange is short compared to the oscillation period for the standard case. But even for μ about 50 d we find oscillations, however, now delayed by an incubation period, that decreases with the time of exchange between the boxes. We consider this to be an indication that at least the tendency to oscillate persists if dilution and mixing is included.

The diurnal variation of the solar zenith angle and the corresponding variation of the photolysis frequencies is another perturbation that exists in the real atmosphere. In figure 8 the results for NO under an accordingly modified standard case is displayed.

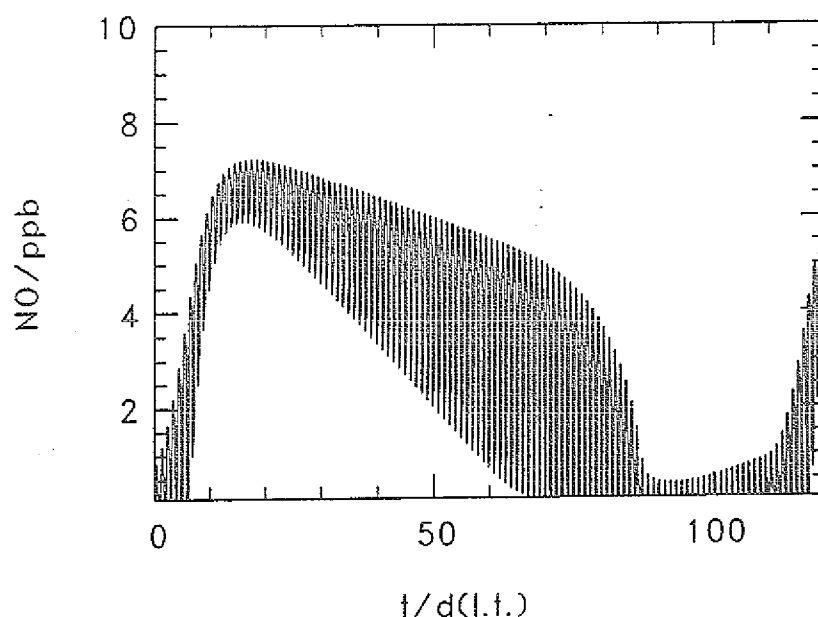


Figure 8: Time dependence of the mixing ratio of NO for the standard case. $Q(\text{NO}) = 10^6 \text{ cm}^3 \text{ s}^{-1}$, $Q(\text{CO}) = 1.3 \cdot 10^6 \text{ cm}^3 \text{ s}^{-1}$. The dependence of the photolysis frequencies of R1 and R2 on the solar zenith angle is included.

There is the expected diurnal variation according to the NO production by the photolysis of NO_2 (R1) whose rate depends on the solar zenith angle. The chemistry induced oscillation is still present, however, the period is roughly doubled, since the chemistry stops during night. Moreover, the shape of the oscillation visualized by the envelope of the time dependence of NO has changed. It indicates a nonlinear

interaction between the diurnal cycle and the chemically induced oscillation which is investigated in a forthcoming paper (Lustfeld and Poppe, 1995).

A severe problem arises from sources that have not been included so far. Frequently entrainment of ozone even into the PBL delivers a significant contribution to the local budget. Since nearly complete depletion of ozone is a genuine part of the oscillatory cycle even small sources $Q(O_3) > 3 \cdot 10^5 \text{ cm}^{-3}\text{s}^{-1}$ inhibit the oscillation for the standard case. For example, exchange on the time scale of days and weeks with air masses containing 50 ppb O_3 would provide such a source.

Additional chemistry can also destroy the oscillatory behaviour. The degradation of methane, which is present everywhere, opens a generically new channel of CO formation. Adopting a steady state approximation for the intermediates HCHO and CH_3O_2 , we describe it simply by



The methane oxidation provides a CO source whose strength is not constant but depends on the OH concentration. Assuming that the reaction above is the dominant CO source the rate equation for CO reads

$$d[CO]/dt = k_{11} [OH][CH_4] - k_9 [OH][CO]. \quad (10)$$

Changing the independent variable to the time integral of the OH concentration (denoted by t') and assuming temporally constant methane we have

$$d[CO]/dt' = k_{11} [CH_4] - k_9 [CO] \quad (11)$$

Carbon monoxide approaches its steady state value $[CO]_s = k_{11} [CH_4]/k_9$ monotonically in time with a simple exponential dependence on t' . The numerical calculation (figure 9) that includes R11 confirms this result. Starting from the ambient methane mixing ratio of 1.7 ppm the oscillation in the standard case are suppressed as long as the mixing ratio of methane exceeds 10 ppb. Below this threshold the

known oscillation in the $\text{CO-O}_3\text{-NO}_x\text{-HO}_x$ system begins to govern the chemical dynamics.

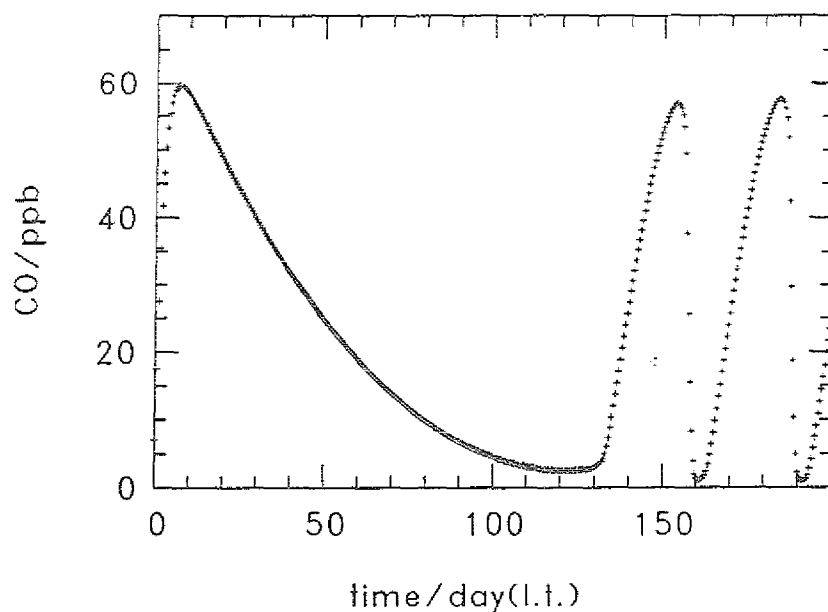


Figure 9: Time dependence of the mixing ratio of CO for the standard case in the presence of methane. $[\text{CH}_4(t=0)] = 1.7 \text{ ppm}$. $Q(\text{NO}) = 10^6 \text{ cm}^3 \text{ s}^{-1}$, $Q(\text{CO}) = 1.3 \cdot 10^6 \text{ cm}^3 \text{ s}^{-1}$.

Note however, that on the much larger time scale of methane another oscillation evolves, where CH_4 takes over the role of CO. This will be discussed in a forthcoming paper (Poppe, 1995).

6. Summary and Conclusions

An oscillatory time dependence has been observed in zerodimensional calculations for a simplified atmospheric chemistry under the influence of fixed sources for CO and NO. The oscillation with a period of days to weeks is a consequence of the nonlinear couplings in the kinetic equations of the system. Prerequisites are comparable source strengths for CO and NO above a threshold value. Though the oscillation is in many respects a stable attractor of the system, it can easily be

perturbed by entrainment of ozone. The degradation of methane forming CO with a rate that depends on the OH concentration, is another effect, that destroys the oscillation. It can be shown, however, that on the time scale of methane another period of several years evolves, where methane takes over the role of CO.

Whether oscillatory behaviour is observable in the real atmosphere is still an open question. Our analysis provides evidence, that at least parts of the stable oscillatory orbit may very well be attained under appropriate conditions.

Acknowledgement

The authors are grateful to D.H. Ehhalt for many fruitful and stimulating discussions during all stages of the work.

References:

Gray, P. and S. K. Scott, Chemical oscillations and instabilities, non-linear chemical kinetics, Clarendon Press, Oxford, 1994.

Kasting, J. F. and T. P. Ackerman, High atmospheric NO_x levels and multiple photochemical steady states, *J. Atmos. Chem.* 3, 321-340, 1985.

Lustfeld, H. and D. Poppe, to be published, 1995.

Madronich, S. and P. Hess, The oxidizing capacity of the troposphere and its changes, in: G. Angeletti and G. Restelli (eds.): Physico-chemical behaviour of atmospheric pollutants, Proceedings of the 6. European symposium, Varese, October 1993, Luxemburg 1994.

Poppe, D., Oscillating methane concentrations from nonlinear gas phase chemistry, to be published 1995.

White, W. H. and D. Dietz, Does the photochemistry of the troposphere admit more than one steady state?, *Nature*, 309, 242-244, 1984.

Zimmermann, J. and D. Poppe, Nonlinear couplings in the tropospheric NO_x - HO_x gas phase chemistry, *J. Atmos. Chem.* 17, 141-155, 1993.

Jül-3011
December 1994
ISSN 0944-2952